Surface chemistry of alanine on Ni{111}

Article

Accepted Version

THE JOURNAL OF PHYSICAL CHEMISTRY C

Article

pubs.acs.org/JPCC

Surface Chemistry of Alanine on Ni{111}

Richard E. J. Nicklin,[†] Alix Cornish,[†] Andrey Shavorskiy,[‡] Silvia Baldanza,[†] Karina Schulte,[§] Zhi Liu,[‡] Roger A. Bennett,[†] and Georg Held*[,†,∥]

[†]Department of Chemistry, University of Reading, Reading RG6 6AD, U.K.

[‡]Advanced Light Source, Lawrence Berkeley National Laboratory, Berkeley, California 94720, United States

[§]MAX-lab, Lund University, 22100 Lund, Sweden

[∥]Diamond Light Source Ltd, Oxfordshire OX11 0DE, U.K.

Supporting Information

ABSTRACT: The adsorption of L-alanine on Ni{111} has been studied as a model of enantioselective heterogeneous catalysts. Synchrotron-based X-ray photoelectron spectroscopy and near-edge X-ray absorption fine structure (NEXAFS) spectroscopy were used to determine the chemical state, bond coordination, and out-of-plane orientation of the molecule on the surface. Alanine adsorbs in anionic and zwitterionic forms between 250 and ≈320 K. NEXAFS spectra exhibit a strong angular dependence of the π^* resonance associated with the carboxylate group, which is compatible with two distinct orientations with respect to the surface corresponding to the bidentate and tridentate binding modes. Desorption and decomposition begin together at ≈300 K, with decomposition occurring in a multistep process up to ≈450 K. Comparison with previous studies of amino acid adsorption on metal surfaces shows that this is among the lowest decomposition temperatures found so far and lower than typical temperatures used for hydrogenation reactions where modified Ni catalysts are used.

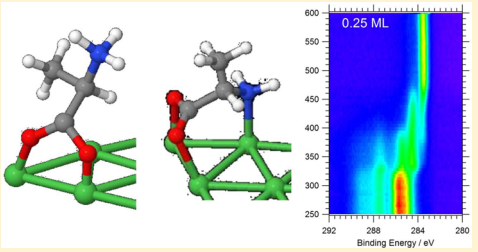

INTRODUCTION

Amino acid adsorption on metals is a burgeoning field of research due to its relevance to chemical sensing, biomedical research, and enantioselective catalysis. Heterogeneous enantioselective catalysis using alanine as a chiral modifier for Ni has been known since 1962.[1] The best studied reaction in this context is the enantioselective hydrogenation of methyl acetoacetate,[2−4] with surface sensitivity results pointing to the involvement of the low-Miller-index planes.[5,6]

The orientation and bonding of amino acids on transition-metal surfaces has been probed by a variety of techniques, notably low-energy electron diffraction (LEED), temperature-programmed desorption (TPD), near-edge X-ray absorption fine structure (NEXAFS) spectroscopy, reflection absorption IR spectroscopy (RAIRS), high-resolution electron energy loss spectroscopy (HREELS), photoelectron diffraction (PhD), scanning tunneling microscopy (STM), and X-ray photoelectron spectroscopy (XPS).[7−47] LEED, NEXAFS, STM, XPS, and PhD have been used to investigate the adsorption of glycine and alanine on Cu surfaces. It was demonstrated that the adsorbate binds as the anion, adopting a tridentate binding mode on the surface, with single Cu atoms bonding to both O atoms and the N atom.[11,19,21,28,46,47] This three-point binding has received theoretical support.[28,48−51] It breaks the surface symmetry and imposes a chiral environment on the surface, a prerequisite for chiral catalysis.[7,52,53] For adsorption on Ni{111}, however, the work by Ghiringhelli et al.[54] suggests that alanine will adsorb via the N atom and a single carboxyl group O atom (the other O atom being protonated). Recent work by Baldanza et al.[45] has highlighted the possibility of a bidentate binding mode for alanine on the Cu{111} surface, where the alanine adsorbs on the surface as the zwitterion, with single Cu atoms bonding to the two O atoms only.

The present work examines the chemical nature and orientation of the smallest chiral modifier, alanine, bound to the Ni{111} surface. Synchrotron-based XPS and NEXAFS spectroscopy are used to determine the chemical state and out-of-plane orientation of the adsorbed molecules. Temperature-programmed (TP-)XPS experiments were performed to investigate changes in the chemical state and decomposition pathways followed by the molecules upon annealing. The experimental results indicate that alanine initially adsorbs in its anionic form with a tridentate binding mode at low coverages. With increasing coverage, alanine begins to bind as the zwitterion in a bidentate mode, with surface saturation at 0.25 ML and both forms of alanine coexisting on the surface. Desorption and decomposition are seen to begin together at around 300 K, with decomposition occurring in a multistep process below 450 K. NEXAFS spectra exhibit strong angular dependence of the π^* resonances associated with the carboxylate group, allowing the establishment of two distinct orientations with respect to the surface, which are presumed to correspond to the bidentate and tridentate binding modes.

Received: September 9, 2015
Revised: October 26, 2015

DOI: 10.1021/acs.jpcc.5b08814
J. Phys. Chem. C XXXX, XXX, XXX−XXX

EXPERIMENTAL SECTION

The experiments were carried out in two different ultrahigh vacuum (UHV) systems. XPS and NEXAFS experiments were performed at both the UHV endstation of beamline I-311 at the MAXlab Synchrotron Radiation Facility in Lund, Sweden,[55] and the near-ambient pressure endstation of beamline 9.3.2 at the ALS Synchrotron in Berkeley, CA, USA,[56] which are equipped with Scienta SES200 and 4000R-Hipp electron energy analysers, respectively.

Standard procedures including Ar^+ ion sputtering and a final annealing step to 1000 K in UHV were applied for sample cleaning. Cleanliness was checked by XPS. The sample temperature was measured by means of K-type thermocouples spot-welded to the sample. L-Alanine (>98% from Aldrich) was dosed by using a home-built evaporator for organic molecules. The evaporator design consists of one or more resistively heated stainless steel crucibles each containing a glass tube filled with the organic material to be evaporated. K-type thermocouples are attached to the crucibles for accurate and reproducible temperature control. L-Alanine was dosed by heating the crucible to temperatures between 413 and 428 K.

For the experiments performed at MAXLab and ALS, L-alanine was adsorbed at sample temperatures of 250 and 300 K, respectively. XP spectra in the C 1s, N 1s, and O 1s regions were recorded using photon energies of 410, 525, and 650 eV, respectively, and a pass energy of 50 eV. Spectra of the Fermi edge were measured after each change in the beamline settings with the same monochromator and analyzer parameters (photon energy, pass energy) to calibrate the offset of the binding energies. In order to study the temperature dependence of the absorbed alanine layers, fast XP spectra were recorded at a rate of typically 27 s per spectrum while annealing the sample at a constant rate of 0.2 K s^{-1} (5.4 K per spectrum).

NEXAFS spectra at the O, C, and N K-edges were recorded at MAXlab in Auger-yield mode using the same analyzer as for XPS and with the photon beam at angles of 0° or 65° with respect to the surface normal. O, C, and N K-edge spectra were recorded in the kinetic energy ranges 490−525 eV, 250−295 eV, and 365−390 eV, while the photon energy was scanned from 525 to 560 eV, 280 to 310 eV, and 395 to 415 eV, respectively, in steps of 0.15 eV. The photon flux, I_0, was recorded by measuring the current from a photodiode inserted into the beamline. NEXAFS spectra were measured for the clean surface and after adsorption of L-alanine at 250 K. The data presented here are integrated over a smaller kinetic energy range of 511.3−513.3 eV (262.5−265.0 eV, 380.5−383.5 eV) in order to avoid artificial structures due to photoemission peaks. These spectra are then divided by I_0, normalized with respect to the pre-edge (low photon energy) background, and have the clean-surface spectra subtracted, which were treated in the same way. In a final step, the spectra were normalized with respect to the postedge (high photon energy) background.

RESULTS AND DISCUSSION

Chemical State. Figure 1 shows the XP spectra recorded in the C 1s, N 1s, and O 1s regions after L-alanine deposition onto the surface at 250 and 300 K. Coverage calibration was performed via comparison of the O 1s and C 1s XPS signal areas with those for a saturated CO layer of known coverage $\Theta = 0.57$ ML[57] using an excitation energy of 950 eV (not shown). With lower photon/kinetic energies, photoelectron (as used for recording the data in Figure 1) diffraction can lead to variations in peak intensities which are not proportional to the surface coverage. The coverage, Θ, is subsequently expressed in terms of L-alanine molecules per surface Ni atom, assuming that all of the carbon and oxygen present on the surface are incorporated in alanine molecules. Strong photoelectron diffraction effects are seen at lower photon energies, with relative peak intensities varying significantly. Whereas previous work on Cu surfaces has shown relatively slight change in overall spectral structure with coverage, the C 1s spectra shown in Figure 1 show notable variation with coverage within the 283−286 eV binding energy envelope. This is attributed to the generation of decomposition fragments at low coverages of alanine, and their presence complicates the fitting of the spectra and the calibration of the surface coverage of intact alanine.

Figure 1a,d shows C 1s spectra recorded after dosing at 250 and 300 K, respectively. Six distinct peaks can be identified at low coverages, with binding energies of 283.5, 284.5, 285.3, 285.7, 287.3, and 288.9−289.1 eV (see Tables S1 and S2 in the Supporting Information for a list of fitting parameters). As coverage increases above 0.11 ML at 250 K (0.20 ML at 300 K), the peak at 285.3 eV appears to shift to 285.0 eV, while, in the multilayer, the peak at 285.7 eV shifts to 286.1 eV. At multilayer coverage, only three peaks can be clearly resolved at 289.1, 287.3, and 286.1 eV. The multilayer is only seen to grow for deposition at 250 K; at 300 K, no multilayer could be generated. The two low binding energy peaks have been assigned to decomposition fragments based on previously published results: atomic carbon or H_xCN are assigned at 283.5 eV[58−60] and −C═C− groups at 284.5 eV.[61−67] The 285.3 eV peaks incongruously high intensity at low coverage, coupled with its apparent movement to 285.0 eV with higher coverage, is consistent with known behavior of CO when coadsorbed with hydrocarbons,[57] although it should be noted that dehydrogenated H_xCN species on Pd{111} also generate a C 1s signal at 285.0 eV.[68] The remaining peaks at 285.7−286.1 eV, 287.3 eV, and 288.9−289.1 eV are assigned in a similar fashion to previous work on Cu{110} and Cu{111}.[28,45] The low coverage 285.7 eV signal is assigned to the superposition of peaks arising from the methyl and α-C atoms in the anionic alaninate. At the multilayer coverage, the methyl C atom peak shifts to 286.1 eV. This shift is a result of reduced screening by the metal in the multilayer as opposed to the monolayer, a similar effect being seen for the carboxylate group shifting from 288.9 to 289.1 eV. The 287.3 eV peak is assigned to the α-C atom of zwitterionic alanine (bound to a $-NH_3$ group).

Figure 1b,e shows N 1s spectra for alanine dosed onto the Ni surface at 250 and 300 K, respectively. Three peaks are observed, at 397.2 eV (only at 300 K), 399.7 eV, and 401.6 eV. These peaks are assigned to a H_xCN decomposition species, $-NH_2$ from anionic alaninate and $-NH_3^+$ from zwitterionic alanine.

The O 1s spectra of Figure 1c,f shows two chemical environments, a dominant peak at 531.5 eV and a small feature at 533.5 eV. These are assigned to the deprotonated carboxylic acid group and the protonated −COOH, respectively.[41] The peak at 533.5 eV is only presented above 0.11 ML at 250 K and above 0.19 ML at 300 K. It is likely that its presence is connected to the abundance of hydrogen on the surface. For submonolayer coverages (i.e., <0.25 ML), the 533.5 eV peak appears to have a fixed relative intensity of 10% of the main peak at 531.5 eV, suggesting a degree of hydrogen bonding between the adsorbed molecules. At coverages above 0.25 ML, the O 1s signal shifts to progressively higher binding energies, indicating the decoupling of the carboxylate group from the surface and the formation of the multilayer. The relative intensity of the 533.5 eV signal also

DOI: 10.1021/acs.jpcc.5b08814
J. Phys. Chem. C XXXX, XXX, XXX−XXX

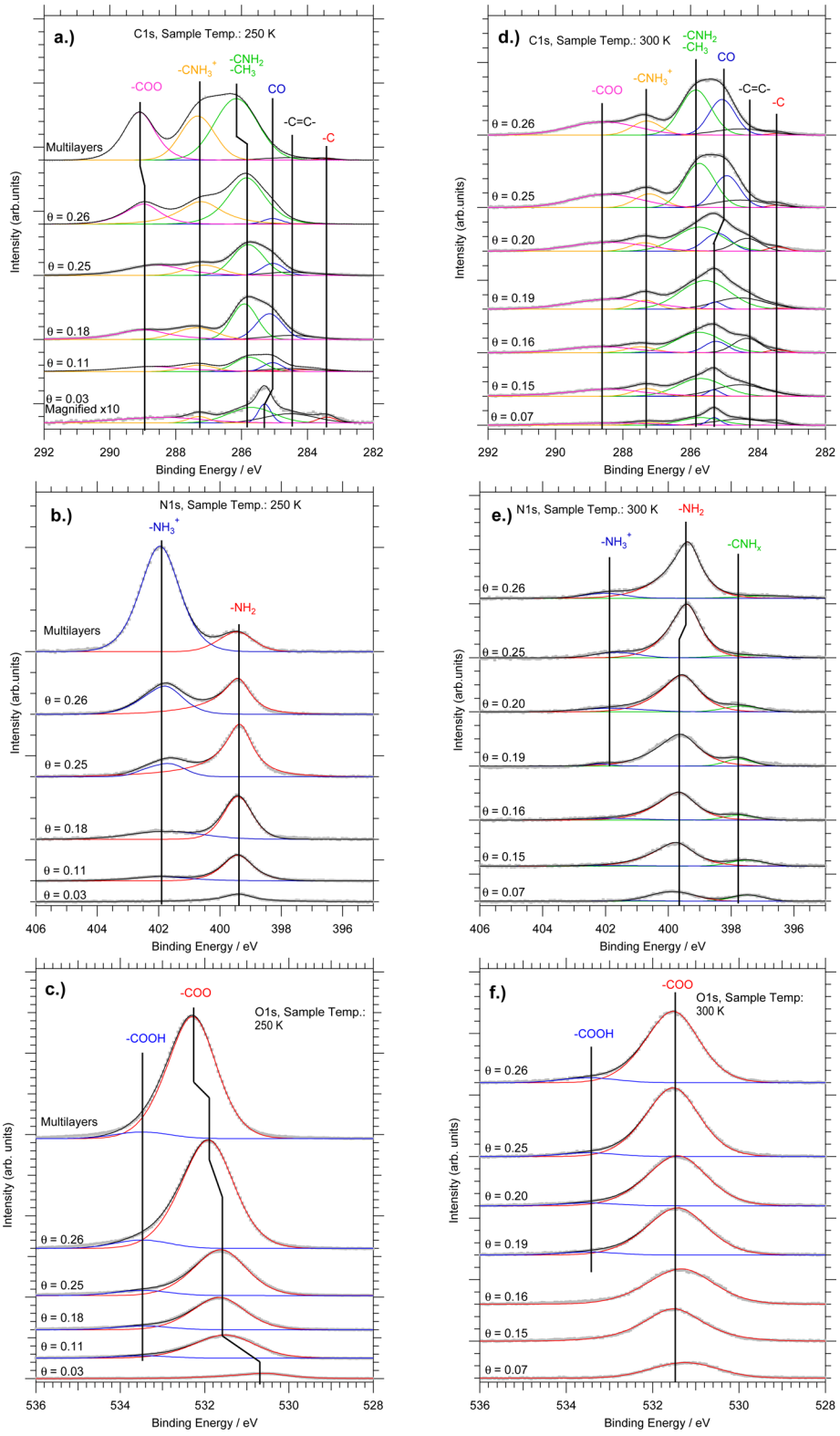

Figure 1. C 1s (a, d), N 1s (b, e), and O 1s (c, f) XP spectra of L-alanine overlayers on Ni{111}, recorded at 410, 525, and 650 eV, respectively. Gray dots represent raw data and continuous lines fitted peaks. Spectra (a–c) adsorbate dosed onto crystal held at 250 K, and (d–f) adsorbate dosed onto crystal held at 300 K.

decreases at high coverages, which leads to the conclusion that alanine is deprotonated in the multilayer. Throughout this discussion, it is assumed that the O 1s signal generated by coadsorbed CO is masked by the intensity of the signal generated by the alanine.

Figure 2 shows a plot of peak areas (in terms of surface coverage) of the C 1s and N 1s peaks discussed above against the total alanine surface coverage for adsorption at 250 K. The 287.3 eV C 1s peak and the 401.6 eV N 1s peak, which are both associated with zwitterionic alanine, are observed

DOI: 10.1021/acs.jpcc.5b08814
J. Phys. Chem. C XXXX, XXX, XXX−XXX

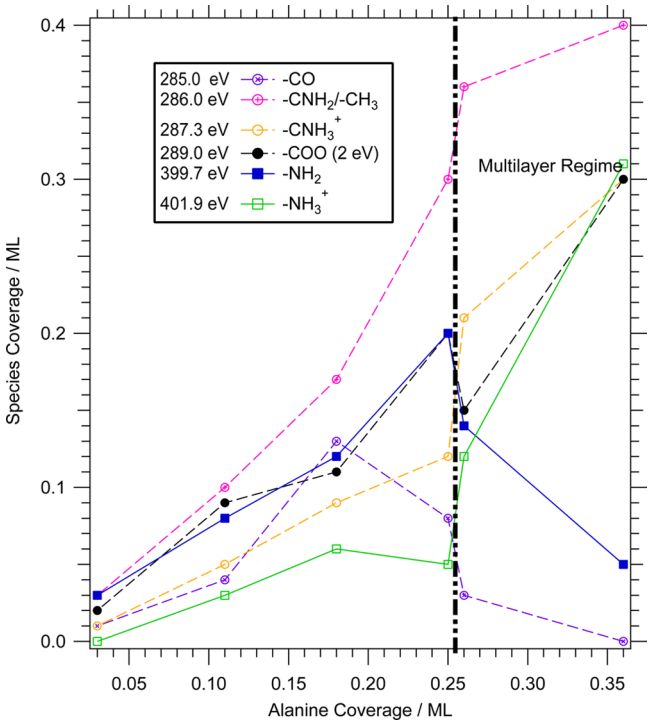

Figure 2. Plot of peak area converted to surface coverage for identified chemical species at varying alanine coverages.

well below the onset of multilayer growth. This raises three possibilities:

- Decomposition fragments are coadsorbed at submonolayer coverages, generating XP signals overlapping with these two peaks.
- A second L-alanine layer begins to grow on the surface before completion of the first chemisorbed layer, producing the NH_3^+ signal from localized multilayers, as suggested by Tysoe for the L-alanine Pd{111} system.[33]
- Bidentate, zwitterionic alanine is present on the surface at temperatures above 250 K, in contrast to alanine on Cu{111}, where the bidentate form has only been observed at 200 K.[45]

It appears unlikely that a decomposition product would mimic the zwitterion quite so precisely. On the other hand, the presence of the 287.3 eV peak at very low surface coverages forces us to consider that a fragment may, in fact, be the dominant contributor to this peak in this coverage regime at temperatures above 320 K. Considering the question of multilayer growth before completion of the monolayer, it is noted that the 401.6 eV peak (associated with the zwitterion) begins to grow in the N 1s XP spectrum at below Θ = 0.11 ML. It seems unlikely that a second layer would begin to form at such a low coverage; however, above Θ = 0.26 ML, the 399.7 eV peak begins to shrink compared to the 401.2 eV peak, suggesting the growth of a second layer over the monolayer, attenuating the 399.7 eV peak signal. We, therefore, favor the third possibility that molecules bound to the surface exist in both the bidentate zwitterionic and the tridentate anionic states at coverages above 0.11 ML, with the anionic state being populated first, and second layers beginning to grow at coverages $\geq$ 0.25 ML. Consequently, it is suggested that 0.25 ML corresponds to the saturation coverage for Ni{111}. This value is supported by the observation of a (2×2) LEED pattern for a saturated glycine layer on Pt{111}[44] and a (2×2)-like for a saturated layer of alanine on Cu{111} observed by STM.[69] It should be noted, however, that no superstructure was observed in LEED for any of the L-alanine layers on Ni{111} prepared in this work.

Molecular Orientation. Figure 3 shows O and N K-edge NEXAFS spectra of alanine layers on Ni{111} close to saturation coverage (Θ = 0.25 ML) recorded at 250 K with the X-ray beam at 0° and 65° with respect the surface normal. Carbon K-edge NEXAFS data were also recorded (see the Supporting Information); however, strong background features overlapping with the adsorbate signal do not allow a quantitative analysis of these spectra.

The oxygen K-edge spectra (Figure 3a,b) exhibit four peaks. The π^* resonance consists of two peaks at 532.1 and 532.9 eV, which are attributed to COO groups of intact alanine in two different conformations. Figure 3b highlights the fact that the maximum of the π^* resonance is blue-shifted by 0.15 eV from the 65° to the 0° spectra, confirming that the resonance consists of two distinct peaks with different angle dependencies. The angular dependencies of the high and low energy peaks, respectively, return tilt angles of the COO groups of 56° and 64° to the surface (see the Supporting Information and ref 70 for details). In addition, two broad σ resonances can be resolved at 539.0 and 543.2 eV, which are attributed to C−C and C−O bonds in accordance with the assignments made for glycine and alanine on Cu{110}.[19,28]

Figure 3c shows nitrogen K-edge NEXAFS spectra. The main peak at 405.5 eV is assigned to a σ(C-N) shape resonance.[19,28,45] The weak peak at 399.5 eV is assigned to a π^* transition of C═N decomposition fragments, in agreement with prior work identifying X-ray induced decomposition fragments of amino acids.[28,71,72] Such low energy peaks are also seen to develop as alanine-covered Cu surfaces are annealed.[42]

A broad conclusion from these NEXAFS data is that alanine is adsorbed on the surface in two conformations discriminated by differing tilt angles of the COO plane. It is presumed that these two conformations correspond to tridentate (low tilt angle) and bidentate (high tilt angle) adsorption.

Temperature Dependence. Figure 4 summarizes the temperature-programmed XPS experiments examining the behavior of adsorbed alanine during annealing. The TP-XPS diagrams (Figure 4a−c) comprise a series of fast XP spectra recorded as the temperature of the sample was ramped at 0.2 K s^{-1} (5.4 K per spectrum; for examples, see Figure 4d−f) and merged to produce a 2D plot of temperature vs binding energy, where false color is used to show spectrum intensity. Vertical line profiles taken at fixed binding energies are shown to illustrate the evolution of the chemical state of the adsorbed alanine (Figure 4g−i).

The behavior starting from multilayer coverage (>0.4 ML), dosed at 200 K, is tracked through the N 1s spectra in Figure 4a,d,g, while the N 1s and C 1s spectra in Figure 4b,e,h and c,f,i show the behavior of the saturated chemisorbed layer (Θ = 0.25 ML) dosed at 250 K. Significant changes take place between 300 and 480 K. Complete decomposition of surface-bound alanine is associated with the appearance of C 1s and N 1s peaks at around 283.5 and 397.2 eV, respectively. Alanine desorption commences at around 300 K, as the N 1s peak at binding energy 399.7 eV and the C 1s peaks at 286.0 and 289.0 eV, previously assigned to intact alanine, decrease dramatically, initially without a corresponding growth of the peaks assigned to decomposition products. Decomposition starts at around 320 K and proceeds to

DOI: 10.1021/acs.jpcc.5b08814
J. Phys. Chem. C XXXX, XXX, XXX−XXX

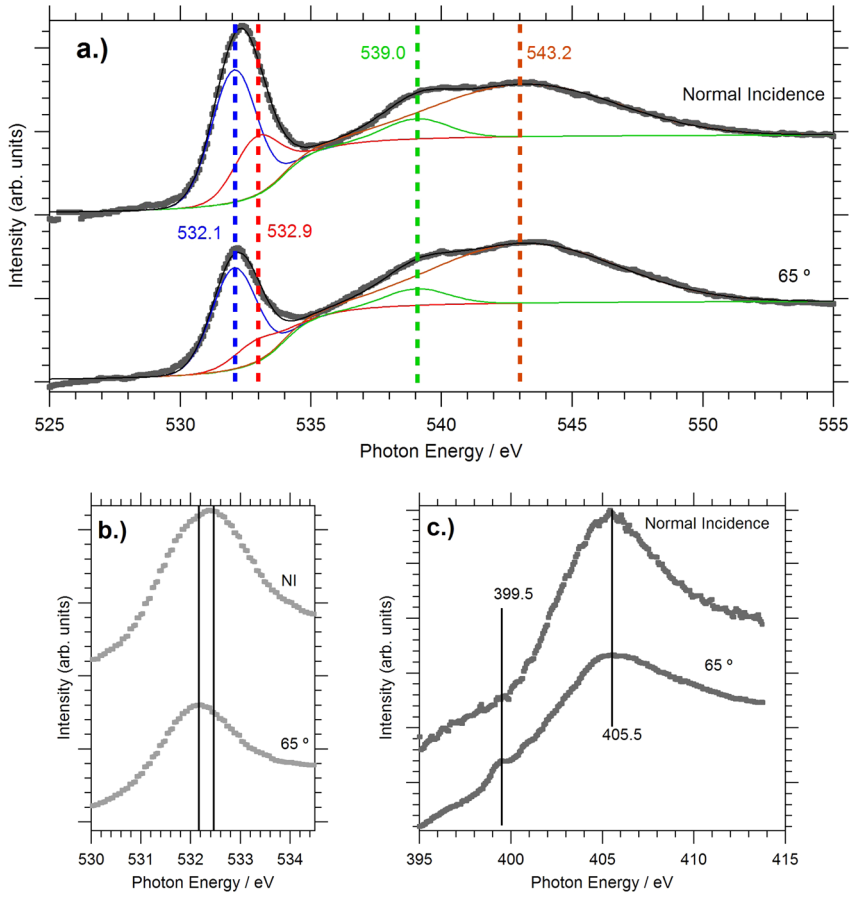

Figure 3. Experimental data (dots) and fits (lines) of Auger yield NEXAFS (a, b: O K-edge data; c: N K-edge data) for a saturated layer of L-alanine on Ni{111} at 250 K. Angles indicated are those between the surface normal and the X-ray beam.

completion in at least three steps at ≈320 K, ≈380 K, and ≈460 K, which are most clearly seen in the C 1s spectrum (Figure 4b,h). Above 480 K, the N 1s and C 1s signals cease to change in binding energy or intensity until they disappear completely at ≈730 K.

Temperature-programmed desorption experiments (see the Supporting Information) show evolution of H_2 and CO_2 between 300 and 450 K with two peaks at 350 and 420 K and two desorption peaks of relative mass 28, which are assigned to CO (420 K) and N_2 (570 K). Considering the higher heating rate in the TPD experiments (1 K s^{-1}), the desorption/decomposition processes are expected to be shifted to higher temperatures. We, therefore, correlate the TPD peaks to the changes observed in TP-XPS as follows: 350 K (TPD) ↔ 320 K (TP-XPS), 420 K (TPD) ↔ 380 K (TP-XPS), 570 K (TPD) ↔ 460 K (TP-XPS). The assignment of the mass 28 TPD peaks is based on the observation that there is no oxygen signal visible in XPS above 400 K, whereas a desorption of a small fraction of nitrogen is compatible with the N 1s signal.

The first two decomposition steps include dehydrogenation and lead to the release of hydrogen and the breaking of the C−C "backbone" of the amino acid, which is accompanied by the loss of CO_2. Both processes occur in parallel; however, the different relative intensities in the H_2 and CO_2 desorption features indicate that dehydrogenation dominates in the first step, leaving behind an intermediate, which undergoes C−C bond scission in the second step. Overall, the surface reaction taking place between 300 and 400 K is

$$\mathrm{OOC\text{-}CH(CH_3)(NH_2)_{(ads)}} \rightarrow \mathrm{H_xC_2N_{(ads)}} + \mathrm{CO_{2(g)}} + \left(3 - \frac{x}{2}\right)\mathrm{H_{2(g)}}$$

Figure 4g,h,i shows that the integrated area under the N 1s XPS signal does not change much above 350 K, whereas the integrated C 1s signal falls by more than 50% between 350 and 480 K, supporting the above mechanism. The amine residue will then undergo sequential loss of hydrogen until a highly unsaturated hydrocarbon is left on the surface. This transition causes the changes in binding energy seen around 460 K. Figure 4h shows a drop to 56% in the integrated N 1s signal (1/1.8 of the initial intensity) for the saturated chemisorbed layer between 300 and 500 K, whereas the integrated C 1s drops to 34% (1/2.9 in Figure 4i). Considering that the C:N ratio for intact alanine (at 300 K) is 3:1 and disregarding possible intensity variations due to diffraction effects, this would lead to a C:N ratio of 2:1 after complete decomposition. The C 1s and N 1s signals of the decomposition products disappear at the same temperature, 730 K (N_2 desorbs into the gas phase, and C dissolves into the Ni bulk). This is a strong indication that the C and N atoms are still associated in a molecular surface species at higher temperatures rather than isolated chemisorbed atoms. Additional support for this assumption comes from the fact that the nitrogen K-edge NEXAFS spectrum of this species is different from published spectra of atomic N on Ni surfaces (see Figure S2 in the Supporting Information and ref 73). An extended N-doped

DOI: 10.1021/acs.jpcc.5b08814
J. Phys. Chem. C XXXX, XXX, XXX−XXX

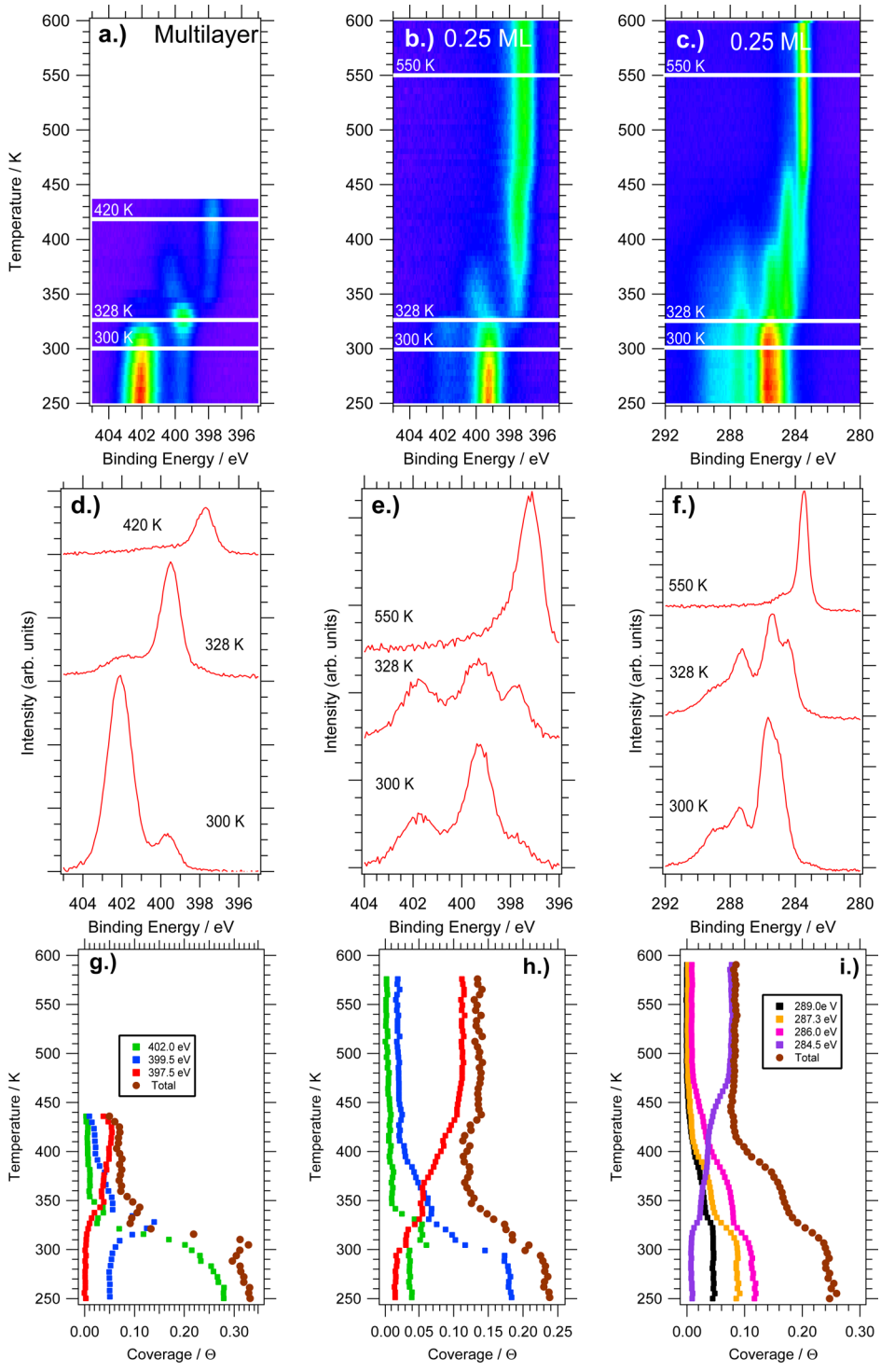

Figure 4. (a–c) TP-XPS data for L-alanine adsorbed on Ni{111}, (d–f) selected spectra extracted from (a–c), (g–i) integrated line profiles showing integrated intensity in 2 eV wide bands. (a, d, g) N 1s (excitation energy 525 eV) of >0.4 ML dosed at 200 K. (b, e, h) N 1s (excitation energy 525 eV) of 0.25 ML dosed at 250 K. (c.) C 1s (excitation energy 410 eV) of 0.25 ML dosed at 250 K. Heating rate β = 0.2 K s^{-1}; data acquisition time per spectrum, 27 s.

graphene-like C_y-N network can be excluded as the XPS binding energies reported for such structures are in the ranges of 284.5–285.0 eV (C 1s) and 398.7–400.7 eV (N 1s), i.e., significantly higher than the ones found here, and they are stable up to >900 K.[74]

CONCLUSIONS AND SUMMARY

Thermal decomposition of small amino acids, such as alanine and glycine, has previously been observed on a suite of surfaces by means of TPD and TP-XPS, including Cu{111},[45] Cu{110},[7,42] Cu{531},[39] Pt{111},[41,44] and Pd{111}.[32,33] In all surveyed cases, decomposition proceeds via a β-hydride elimination step (or possibly γ-elimination in the case of alanine) prior to C–C bond scission between the carboxylate and the α-carbon, which leads to the release of H_2 and CO_2 into the gas phase. This is followed by sequential dehydrogenation and collapse of the alkyl amine, releasing H_2 into the gas phase. From the list of decomposition temperatures in Table 1, it is clear that Ala/Ni{111}, alongside

DOI: 10.1021/acs.jpcc.5b08814
J. Phys. Chem. C XXXX, XXX, XXX–XXX

Table 1. Onset of Decomposition for Glycine and Alanine Adsorbed on Different Single Crystal Surfaces under UHV Conditions

	onset (K)	method	ref
Ala/Cu{111}	440	TPD	45
	425	TP-XPS	45
Ala/Cu{110}	500	TPD	7
	470	TP-XPS	42
Ala/Ni{111}	320	TP-XPS	this work
Ala/Pd{111}	350	TPD	33
Gly/Cu{110}	460	TP-XPS	42
Gly/Cu{531}	490	TPD	39
Gly/Pd{111}	320	TPD	32
Gly/Pt{111}	360	TPD	44
	350	TP-XPS	41

Gly/Pd{111}, is among the least stable adsorption systems studied so far. The onset of decomposition around 320 K is more than 100 K lower than that for the close-packed Cu{111} surface. In general, dissociation is far more facile on the group-10 transition metals than on Cu. Therefore, Cu surfaces are not likely to be good models for enantioselective modification of the Ni, Pd, or Pt catalysts that are used in enantioselective hydrogenation reactions. Important in this context is also the fact that the onset of decomposition for Ala/Ni{111} is within the range of temperatures used for chiral modification of Raney nickel (273−373 K) and below the typical range of reaction temperatures for the enantioselective hydrogenation of MAA (333−343 K).[2,3] This is a clear indication that the active modifier under reaction conditions is not the intact alaninate surface species that we observed below 320 K in UHV in the present study. Under reaction conditions, decomposition of alanine may be hindered by the presence of solvent and/or the reactants on the surface; however, this would almost certainly also involve a change in the geometry and bond coordination of the adsorption complex. A recent near-ambient pressure study of Gly/Pt{111} has shown that an aqueous environment up to 0.2 Torr does not stabilize the intact adsorbate on this system significantly, although the stability and reaction path of the decomposition products change.[41] Payne et al.[75] have shown that exposure to water vapor in the range of 10^9 L (= 10^3 mbar s) leads to significant surface oxidation on polycrystalline Ni samples, as one would also expect under catalytic reaction conditions.[76] Neither the behavior of relevant chiral molecules on Ni oxides nor the influence of other solvents or the reactants of the hydrogenation reaction on the surface chemistry of amino acids have been studied so far. Another possibility is that the $H_xC_2N_{(ads)}$ surface species resulting from the first decomposition step is the actual modifier. This species is not chiral, but it could stabilize a chiral reconstruction of the Ni surface and/or form a chiral complex with the solvent or one of the reactants.

In summary, the chemical sate and molecular orientation of L-alanine on Ni{111} have been investigated between 250 and 600 K. Synchrotron-based XPS and NEXAFS spectroscopy show that alanine is adsorbed in both the anionic (tridentate) and the zwitterionic (bidentate) states up to room temperature, with both states coexisting in the saturated layer. The chemisorbed layer saturates at $\Theta = 0.25$ ML. At low coverages, decomposition of the alanine molecule is significant even at 250 K; however, at higher coverages, surface congestion appears to prevent break up of the molecule. Desorption and decomposition begin together at ≈300 K, with decomposition occurring in a multistep process up to 450 K.

■ ASSOCIATED CONTENT

Supporting Information

The Supporting Information is available free of charge on the ACS Publications website at DOI: 10.1021/acs.jpcc.5b08814.

Data analysis and additional data (PDF)

■ AUTHOR INFORMATION

Corresponding Author

*Phone: +44 (0)118 3784367. Fax: +44 (0)118 3786331. E-mail: g.held@reading.ac.uk.

Notes

The authors declare no competing financial interest.

■ ACKNOWLEDGMENTS

The research leading to these results has received funding from the U.K.'s EPSRC through grants EP/G068593/1 and EP/F02116X/1, the European Community's Seventh Framework Programme (FP7/2007-2013) CALIPSO under grant agreement No. 312284, and the Marie Curie Training Network SMALL funded by the European Community's Seventh Framework under grant agreement No. 238804. The authors thank the staff of ALS and MAXlab for their help during the experiments.

■ REFERENCES

(1) Fukawa, H.; Izumi, Y.; Komatsu, S.; Akabori, S. Studies on modified hydrogenation catalyst. I. Selective hydrogenation activity of modified Raney nickel catalyst for carbonyl group and C═C double bond. *Bull. Chem. Soc. Jpn.* **1962**, *35*, 1703−1706.

(2) Izumi, Y. Modified Raney Nickel (MRNi) Catalyst: Heterogeneous enantio-differentiating (asymmetric) catalyst. *Adv. Catal.* **1983**, *32*, 215−271.

(3) Keane, M. A. Adsorption of optically pure alanine on silica-supported nickel and the consequent catalytic enantioselectivity. *Langmuir* **1994**, *10*, 4560−4565.

(4) Baddeley, C. J. Fundamental investigations of enantioselective heterogeneous catalysis. *Top. Catal.* **2003**, *25*, 17−28.

(5) Nitta, Y.; Sekine, F.; Imanaka, T.; Teranishi, S. The effect of crystallite size of nickel on the enantioselectivity of modified nickel catalysts. *Bull. Chem. Soc. Jpn.* **1981**, *54*, 980−984.

(6) Wolfson, A.; Geresh, S.; Landau, M. V.; Herskowitz, M. Enantioselective hydrogenation of methyl acetoacetate catalyzed by nickel supported on activated carbon or graphite. *Appl. Catal., A* **2001**, *208*, 91−98.

(7) Barlow, S. M.; Louafi, S.; Le Roux, D.; Williams, J.; Muryn, C.; Haq, S.; Raval, R. Polymorphism in supramolecular chiral structures of R- and S-alanine on Cu(110). *Surf. Sci.* **2005**, *590*, 243−263.

(8) Williams, J.; Haq, S.; Raval, R. The bonding and orientation of the amino acid L-alanine on Cu{110} determined by RAIRS. *Surf. Sci.* **1996**, *368*, 303−309.

(9) Löfgren, P.; Krozer, A.; Lausmaa, J.; Kasemo, B. Glycine on Pt(111): a TDS and XPS study. *Surf. Sci.* **1997**, *370*, 277−292.

(10) Barlow, S. M.; Kitching, K. J.; Haq, S.; Richardson, N. V. A study of glycine adsorption on a Cu{110} surface using RAIRS. *Surf. Sci.* **1998**, *401*, 322−335.

(11) Booth, N. A.; Woodruff, D. P.; Schaff, O.; Gießel, T.; Lindsay, R.; Baumgärtel, P.; Bradshaw, A. M. Determination of the local structure of glycine adsorbed on Cu(110). *Surf. Sci.* **1998**, *397*, 258−264.

(12) Zhao, X.; Rodriguez, J. Photoemission study of glycine adsorption on Cu/Au(111) interfaces. *Surf. Sci.* **2006**, *600*, 2113−2121.

(13) Zhao, X.; Yan, H.; Zhao, R. G.; Yang, W. S. Self-assembled structures of glycine on Cu(111). *Langmuir* **2003**, *19*, 809−813.

DOI: 10.1021/acs.jpcc.5b08814
J. Phys. Chem. C XXXX, XXX, XXX−XXX

(14) Zhao, X.; Gai, Z.; Zhao, R. G.; Yang, W. S.; Sakurai, T. Adsorption of glycine on Cu(001) and related step faceting and bunching. *Surf. Sci.* **1999**, *424*, L347−L351.
(15) Zhao, X.; Zhao, R. G.; Yang, W. S. Adsorption of alanine on Cu(001) studied by scanning tunneling microscopy. *Surf. Sci.* **1999**, *442*, L995−L1000.
(16) Chen, Q.; Frankel, D. J.; Richardson, N. V. Chemisorption induce chirality: glycine on Cu {110}. *Surf. Sci.* **2002**, *497*, 37−46.
(17) Chen, Q.; Frankel, D. J.; Richardson, N. V. The formation of enantiospecific phases on a Cu{110} surface. *PhysChemComm* **1999**, *9*, 41−44.
(18) Kühnle, A.; Linderoth, T. R.; Besenbacher, F. Self-assembly of monodispersed, chiral nanoclusters of cysteine on the Au(110)-(1 × 2) Surface. *J. Am. Chem. Soc.* **2003**, *125*, 14680−14681.
(19) Hasselström, J.; Karis, O.; Weinelt, M.; Wassdahl, N.; Nilsson, A.; Nyberg, M.; Pettersson, L. G. M.; Samant, M. G.; Stöhr, J. The adsorption structure of glycine adsorbed on Cu(110): comparison with formate and acetate/Cu(110). *Surf. Sci.* **1998**, *407*, 221−236.
(20) Nyberg, M.; Hasselström, J.; Karis, O.; Wassdahl, N.; Weinelt, M.; Nilsson, A.; Pettersson, L. G. M. The electronic structure and surface chemistry of glycine adsorbed on Cu(110). *J. Chem. Phys.* **2000**, *112*, 5420−5427.
(21) Sayago, D. I.; Polcik, M.; Nisbet, G.; Lamont, C. L. A.; Woodruff, D. P. Local structure determination of a chiral adsorbate: Alanine on Cu(110). *Surf. Sci.* **2005**, *590*, 76−87.
(22) Gonella, G.; Terreni, S.; Cvetko, D.; Cossaro, A.; Mattera, L.; Cavalleri, O.; Rolandi, R.; Morgante, A.; Floreano, L.; Canepa, M. Ultrahigh vacuum deposition of L-cysteine on Au(110) studied by high-resolution X-ray photoemission: from early stages of adsorption to molecular organization. *J. Phys. Chem. B* **2005**, *109*, 18003−18009.
(23) Ihs, A.; Liedberg, B.; Uvdal, K.; Tornkvist, C.; Bodo, P.; Lundstrom, I. Infrared and photoelectron-spectroscopy of amino-acids on copper - glycine, L-alanine and beta-alanine. *J. Colloid Interface Sci.* **1990**, *140*, 192−206.
(24) Uvdal, P.; Bodo, P.; Liedberg, B. L-cysteine adsorbed on gold and copper - an X-ray photoelectron-spectroscopy study. *J. Colloid Interface Sci.* **1992**, *149*, 162−173.
(25) Iwai, H.; Egawa, C. Molecular orientation and intermolecular interaction in alanine on Cu(001). *Langmuir* **2010**, *26*, 2294−2300.
(26) Iwai, H.; Tobisawa, M.; Emori, A.; Egawa, C. STM study of D-alanine adsorption on Cu(001). *Surf. Sci.* **2005**, *574*, 214−218.
(27) Gladys, M. J.; Stevens, A. V.; Scott, N. R.; Jones, G.; Batchelor, D.; Held, G. Enantiospecific adsorption of alanine on the chiral Cu(531) surface. *J. Phys. Chem. C* **2007**, *111*, 8331−8336.
(28) Jones, G.; Jones, L. B.; Thibault-Starzyk, F.; Seddon, E. A.; Raval, R.; Jenkins, S. J.; Held, G. The local adsorption geometry and electronic structure of alanine on Cu{110}. *Surf. Sci.* **2006**, *600*, 1924−1935.
(29) Jones, T. E.; Baddeley, C. J.; Gerbi, A.; Savio, L.; Rocca, M.; Vattuone, L. Molecular ordering and adsorbate induced faceting in the Ag110-(S)-glutamic acid system. *Langmuir* **2005**, *21*, 9468−9475.
(30) Jones, T. E.; Urquhart, M. E.; Baddeley, C. J. An investigation of the influence of temperature on the adsorption of the chiral modifier, (S)-glutamic acid, on Ni{111}. *Surf. Sci.* **2005**, *587*, 69−77.
(31) Gao, F.; Wang, Y.; Burkholder, L.; Tysoe, W. T. Chemistry of L-proline on Pd{111}: TPD and XPS study. *Surf. Sci.* **2007**, *601*, 3579−3588.
(32) Gao, F.; Li, Z.; Wang, Y.; Burkholder, L.; Tysoe, W. T. Chemistry of glycine on Pd(111): temperature programmed desorption and X-ray photoelectron spectroscopic study. *J. Phys. Chem. C* **2007**, *111*, 9981−9991.
(33) Gao, F.; Li, Z.; Wang, Y.; Burkholder, L.; Tysoe, W. T. Chemistry of alanine on Pd(111): temperature programmed desorption and X-ray photoelectron spectroscopic study. *Surf. Sci.* **2007**, *601*, 3276−3288.
(34) Mahapatra, M.; Burkholder, L.; Bai, Y.; Garvey, M.; Boscoboinik, J. A.; Hirschmugl, C.; Tysoe, W. T. Formation of chiral self-assembled structures of amino acids on transition-metal surfaces: alanine on Pd (111). *J. Phys. Chem. C* **2014**, *118*, 6856−6865.
(35) Thomsen, L.; Tadich, A.; Riley, D. P.; Cowie, B. C. C.; Gladys, M. J. Investigating the Enantioselectivity of Alanine on a Chiral Cu{421}(R) Surface. *J. Phys. Chem. C* **2012**, *116*, 9472−9480.
(36) Thomsen, L.; Wharmby, M.; Riley, D. P.; Held, G.; Gladys, M. J. The adsorption and stability of sulfur containing amino acids on Cu{531}. *Surf. Sci.* **2009**, *603*, 1253−1261.
(37) Schiffrin, A.; Riemann, A.; Auwärter, W.; Pennec, Y.; Weber-Bargioni, A.; Cvetko, D.; Cossaro, A.; Morgante, A.; Barth, J. V. Zwitterionic self-assembly of L-methionine nanogratings on the Ag(111) surface. *Proc. Natl. Acad. Sci. U. S. A.* **2007**, *104*, 5279−5284.
(38) Eralp, T.; Cornish, A.; Shavorskiy, A.; Held, G. The study of chiral adsorption systems using synchrotron-based structural and spectroscopic techniques: stereospecific adsorption of serine on Au-modified chiral Cu{531} surfaces. *Top. Catal.* **2011**, *54*, 1414−1428.
(39) Eralp, T.; Zheleva, Z. V.; Shavorskiy, A.; Dhanak, V. R.; Held, G. Adsorption geometry of glycine on the intrinsically chiral Cu{531} surface. *Langmuir* **2010**, *26*, 10918−10923.
(40) Eralp, T.; Shavorskiy, A.; Zheleva, Z. V.; Held, G.; Kalashnyk, N.; Ning, Y.; Linderoth, T. R. Global and local chiral resolution of serine on the Cu{110} surface. *Langmuir* **2010**, *26*, 18841−18851.
(41) Shavorskiy, A.; Eralp, T.; Schulte, K.; Bluhm, H.; Held, G. Surface chemistry of glycine on Pt{111} in different aqueous environments. *Surf. Sci.* **2013**, *607*, 10−19.
(42) Shavorskiy, A.; Aksoy, F.; Grass, M. E.; Liu, Z.; Bluhm, H.; Held, G. A step toward the wet surface chemistry of glycine and alanine on Cu{110}: destabilization and decomposition in the presence of near-ambient water vapor. *J. Am. Chem. Soc.* **2011**, *133*, 6659−6667.
(43) Inoue, Y.; Okabe, K.; Yasumori, I. X-ray photoelectron spectra of adsorbed methyl acetoacetate and coordinated tartaric acid, aspartic acid and alanine on the nickel surface. *Bull. Chem. Soc. Jpn.* **1981**, *54*, 613−614.
(44) Ernst, K. H.; Christmann, K. The interaction of glycine with a platinum (111) surface. *Surf. Sci.* **1989**, *224*, 277−310.
(45) Baldanza, S.; Cornish, A.; Nicklin, R. E.; Zheleva, Z. V.; Held, G. Surface chemistry of alanine on Cu{111}: Adsorption geometry and temperature dependence. *Surf. Sci.* **2014**, *629*, 114−122.
(46) Efstathiou, V.; Woodruff, D. Characterisation of the interaction of glycine with Cu(110) and Cu(111). *Surf. Sci.* **2003**, *531*, 304−318.
(47) Kang, J.-H.; Toomes, R. L.; Polcik, M.; Kittel, M.; Hoeft, J.-T.; Efstathiou, V.; Woodruff, D. P.; Bradshaw, A. M. Structural investigation of glycine on Cu(100) and comparison to glycine on Cu(110). *J. Chem. Phys.* **2003**, *118*, 6059−6071.
(48) Rankin, R. B.; Sholl, D. S. First-principles studies of chiral step reconstructions of Cu(100) by adsorbed glycine and alanine. *J. Chem. Phys.* **2006**, *124*, 074703−1−6.
(49) Rankin, R. B.; Sholl, D. S. Assessment of heterochiral and homochiral glycine adlayers on Cu(1 1 0) using density functional theory. *Surf. Sci.* **2004**, *548*, 301−308.
(50) Rankin, R. B.; Sholl, D. S. Structure of enantiopure and racemic alanine adlayers on Cu(110). *Surf. Sci.* **2005**, *574*, L1−L8.
(51) Rankin, R. B.; Sholl, D. S. Structures of glycine, enantiopure alanine, and racemic alanine adlayers on Cu(110) and Cu(100) surfaces. *J. Phys. Chem. B* **2005**, *109*, 16764−16773.
(52) Barlow, S. M.; Raval, R. Complex organic molecules at metal surfaces: bonding, organisation and chirality. *Surf. Sci. Rep.* **2003**, *50*, 201−341.
(53) Raval, R. Nanoscale insights into the creation of chiral surfaces. *J. Mol. Catal. A: Chem.* **2009**, *305*, 112−116.
(54) Ghiringhelli, L. M.; Schravendijk, P.; Delle Site, L. Adsorption of alanine on a Ni(111) surface: A multiscale modeling oriented density functional study. *Phys. Rev. B: Condens. Matter Mater. Phys.* **2006**, *74*, 035437.
(55) Nyholm, R.; Andersen, J. N.; Johansson, U.; Jensen, B. N.; Lindau, I. Beamline I311 at MAX-LAB: a VUV/soft X-ray undulator beamline for high resolution electron spectroscopy. *Nucl. Instrum. Methods Phys. Res., Sect. A* **2001**, *467−468*, 520−524.
(56) Grass, M. E.; Karlsson, P. G.; Aksoy, F.; Lundqvist, M.; Wannberg, B.; Mun, B. S.; Hussain, Z.; Liu, Z. New ambient pressure photoemission

DOI: 10.1021/acs.jpcc.5b08814
J. Phys. Chem. C XXXX, XXX, XXX−XXX

615 endstation at Advanced Light Source beamline 9.3.2. *Rev. Sci. Instrum.*
616 **2010**, *81*, 053106−1−7.
617 (57) Held, G.; Schuler, J.; Sklarek, W.; Steinrück, H.-P. Determination
618 of adsorption sites of pure and coadsorbed CO on Ni(111) by high
619 resolution X-ray photoelectron spectroscopy. *Surf. Sci.* **1998**, *398*, 154−
620 171.
621 (58) Carley, A. F.; Chinn, M.; Parkinson, C. R. The adsorption and
622 oxidation of cyanogen on copper surfaces. *Surf. Sci.* **2003**, *537*, 64−74.
623 (59) Carley, A. F.; Chinn, M.; Parkinson, C. R. Polymerisation of
624 cyanogen on graphite and copper films. *Surf. Sci.* **2002**, *517*, L563−
625 L567.
626 (60) Fleming, G.; Adib, K.; Rodriguez, J.; Barteau, M.; White, J.; Idriss,
627 H. The adsorption and reactions of the amino acid proline on rutile
628 TiO2(1;1;0) surfaces. *Surf. Sci.* **2008**, *602*, 2029−2038.
629 (61) Lorenz, M.; Fuhrmann, T.; Streber, R.; Bayer, A.; Bebensee, F.;
630 Gotterbarm, K.; Kinne, M.; Traenkenschuh, B.; Zhu, J. F.; Papp, C.; et al.
631 Ethene adsorption and dehydrogenation on clean and oxygen
632 precovered Ni(111) studied by high resolution x-ray photoelectron
633 spectroscopy. *J. Chem. Phys.* **2010**, *133*, 014706.
634 (62) Papp, C.; Denecke, R.; Steinrück, H.-P. Adsorption and reaction
635 of cyclohexene on a Ni(111) surface. *Langmuir* **2007**, *23*, 5541−5547.
636 (63) Papp, C.; Fuhrmann, T.; Tränkenschuh, B.; Denecke, R.;
637 Steinrück, H.-P. Kinetic isotope effects and reaction intermediates in the
638 decomposition of methyl on flat and stepped platinum (111) surfaces.
639 *Chem. Phys. Lett.* **2007**, *442*, 176−181.
640 (64) Steinrück, H.-P.; Fuhrmann, T.; Papp, C.; Traenkenschuh, B.;
641 Denecke, R. A detailed analysis of vibrational excitations in X-ray
642 photoelectron spectra of adsorbed small hydrocarbons. *J. Chem. Phys.*
643 **2006**, *125*, 204706.
644 (65) Zhao, Q.; Deng, R.; Zaera, F. Thermal activation and reaction of
645 allyl alcohol on Ni(100). *Surf. Sci.* **2011**, *605*, 1236−1242.
646 (66) Zhao, Q.; Deng, R.; Zaera, F. Formation of an oxametallacycle
647 surface intermediate via thermal activation of 1-chloro-2-methyl-2-
648 propanol on Ni(100). *J. Phys. Chem. C* **2010**, *114*, 7913−7919.
649 (67) Castonguay, M.; Roy, J.-R.; McBreen, P. H. Sequential selective
650 formation of adsorbed tert-butoxy and tert-butyl groups from tert-butyl
651 formate on Ni(111). *Langmuir* **2000**, *16*, 8306−8310.
652 (68) Chen, J. J.; Winograd, N. The adsorption and decomposition of
653 methylamine on Pd{111}. *Surf. Sci.* **1995**, *326*, 285−300.
654 (69) Ge, S.-P.; Lü, C.; Zhao, R.-G. Adsorption of L-alanine on Cu(111)
655 studied by scanning tunnelling microscopy. *Chin. Phys. Lett.* **2006**, *23*,
656 1558−1561.
657 (70) Stöhr, J. *NEXAFS Spectroscopy*; Springer Series in Surface
658 Sciences; Springer: Berlin, 1996.
659 (71) Zubavichus, Y.; Fuchs, O.; Weinhardt, L.; Heske, C.; Umbach, E.;
660 Denlinger, J. D.; Grunze, M. Soft X-ray-induced decomposition of
661 amino acids: An XPS, mass spectrometry, and NEXAFS study. *Radiat.*
662 *Res.* **2004**, *161*, 346−358.
663 (72) Zubavichus, Y.; Shaporenko, A.; Grunze, M.; Zharnikov, M.
664 Innershell absortpion spectroscopy of amino acids at all relevant
665 absorption edges. *J. Phys. Chem. A* **2005**, *109*, 6998−7000.
666 (73) Zdansky, E. O. F.; Nilsson, A.; Tillborg, H.; Björneholm, O.;
667 MÅrtensson, N.; Andersen, J. N.; Nyholm, R. Electronic structure of
668 atomic adsorbates from x-ray-absorption spectroscopy: Threshold
669 effects and higher excited states. *Phys. Rev. B: Condens. Matter Mater.*
670 *Phys.* **1993**, *48*, 2632−2648.
671 (74) Zhao, W.; Höfert, O.; Gotterbarm, K.; Zhu, J.; Papp, C.;
672 Steinrück, H.-P. Production of nitrogen-doped graphene by low-energy
673 nitrogen implantation. *J. Phys. Chem. C* **2012**, *116*, 5062−5066.
674 (75) Payne, B. P.; Biesinger, M. C.; McIntyre, N. S. The study of
675 polycrystalline nickel metal oxidation by water vapour. *J. Electron*
676 *Spectrosc. Relat. Phenom.* **2009**, *175*, 55−65.
677 (76) Sugimura, T.; Matsuda, T.; Osawa, T. Synthesis of optically active
678 methyl 4-(4-biphenylyl)-3-hydroxybutanoate via enantioselective hy-
679 drogenation using a tartaric acid-modified nickel catalyst and
680 recrystallization. *Tetrahedron: Asymmetry* **2009**, *20*, 1877−1880.

DOI: 10.1021/acs.jpcc.5b08814
J. Phys. Chem. C XXXX, XXX, XXX−XXX